Oecologia (2008) 156:287–304
DOI 10.1007/s00442-008-0993-2

POPULATION ECOLOGY - ORIGINAL PAPER

Wavelet analysis of ecological time series

Bernard Cazelles · Mario Chavez · Dominique Berteaux · Frédéric Ménard · Jon Olav Vik · Stéphanie Jenouvrier · Nils C. Stenseth

Received: 22 September 2006 / Accepted: 8 January 2008 / Published online: 6 March 2008

Abstract Wavelet analysis is a powerful tool that is already in use throughout science and engineering. The versatility and attractiveness of the wavelet approach lie in its decomposition properties, principally its time-scale localization. It is especially relevant to the analysis of non-stationary systems, i.e., systems with short-lived transient components, like those observed in ecological systems. Here, we review the basic properties of the wavelet approach for time-series analysis from an ecological perspective. Wavelet decomposition offers several advantages that are discussed in this paper and illustrated by appropriate synthetic and ecological examples. Wavelet analysis is notably free from the assumption of stationarity that makes most methods unsuitable for many ecological time series. Wavelet analysis also permits analysis of the relationships between two signals, and it is especially appropriate for following gradual change in forcing by exogenous variables.

Keywords Ecological time series · Transient dynamics · Non-stationarity · Discontinuities · Wavelets · Wavelet analysis · Wavelet Power Spectrum · Wavelet coherency · Environmental forcing

Communicated by Wolf Mooij.

B. Cazelles
Ecole Normale Supérieure, CNRS UMR 7625, 46 rue d'Ulm, 75230 Paris, France

B. Cazelles (✉)
IRD UR GEODES, 93143 Bondy, France
e-mail: cazelles@biologie.ens.fr

M. Chavez
CHU Pitié-Salpêtrière, LENA – CNRS UPR 640, 75651 Paris, France

D. Berteaux
Canada Research Chair in Conservation of Northern Ecosystems, Université du Québec à Rimouski, Rimouski, QC, Canada G5L 3A1

F. Ménard
Centre de Recherche Halieutique Méditerrannéen et Tropical, IRD, UR 109 THETIS, BP 171, 34203 Sète, France

J. O. Vik · N. C. Stenseth
Centre for Ecological and Evolutionary Synthesis (CEES), Department of Biology, University of Oslo, P.O. Box 1050, Blindern, 0316 Oslo, Norway

S. Jenouvrier
Centre d'Etudes Biologiques de Chizé, CNRS, 79360 Villiers en Bois, France

Introduction

Since Elton's classic works (Elton 1924; Elton and Nicholson 1942), understanding and explaining the causes of quasi-regular multiannual cycles in animal populations have been central issues in ecology. Nowadays, explaining both the characteristics of ecological time series and the dependencies between population time series and environmental series is an important challenge (Buonaccorsi et al. 2001; Cazelles and Stone 2003; Liebhold et al. 2004). The importance of this challenge is emphasized by the increasing evidence that several ecological and population processes are affected by climatic fluctuations (Bjørnstad and Grenfell 2001; Stenseth et al. 2002). In particular, a variety of ecosystems and populations are driven by large-scale climatic oscillations (Forchhammer and Post 2004; Klvana et al. 2004).

In ecological studies, population monitoring often consists of a series of observations on the abundance of the organism (or species) made at equal intervals over a

period of time. Statistical procedures are used to extract information and to identify scales of pattern in the population fluctuations. Most of these statistical methods come from what is generally known as time-series analysis. One of the fundamental tools in time-series analysis is the periodogram or spectrum (Chatfield 1989). The signal (the time series) is decomposed into harmonic components based on Fourier analysis. This can be regarded as a partition of the variance of the series into its different oscillating components with different frequencies (periods). Peaks in the periodogram or in the spectrum indicate which frequencies are contributing the most to the variance of the series. In this manner, periodicities, if present, are detected. Spectral analysis in ecology dates back more than 50 years when Bartlett (1954) analyzed Canadian lynx data in the MacKenzie River area with a periodogram. Spectral approaches have been used frequently in ecology and population dynamics (see Platt and Denman 1975 for a review).

The spectral (or correlation) techniques make the assumption that the statistical properties of the time series do not vary with time, i.e., are stationary. However, ecological processes typically violate the stationarity assumption and there are an increasing number of papers that underline the non-stationary features of population dynamics (Cazelles and Hales 2006). For instance, the dynamics of transients can play a key role in the structure of natural systems (Hastings 2001; Benton et al. 2006). Recent studies have shown that population dynamics can switch between different dynamics at multidecadal scales, triggered by small environmental changes. These regime shifts were observed in the North Pacific ecosystem around 1977 (Hare and Mantua 2000). Regime shifts have also been suggested in other regions, for instance, in sea bird populations (Barbraud and Weimerskirch 2001; Jenouvrier et al. 2005) and in some parts of the marine trophic food web (Reid et al. 2001). Environmental perturbations are not the only mechanisms able to generate complex transients. Nonlinear dynamics with "unstable dynamical sets" can also generate complex and non-stationary dynamics (Cushing et al. 1998; Cazelles 2001; Cazelles et al. 2001). Nevertheless, the more spectacular examples of transient behavior in population dynamics have been documented in epidemiological studies (Cazelles and Hales 2006). Long-term changes in climate, human demography and/or social features of human populations have large effects on the dynamics of numerous epidemics as underlined by the analyses of some large data sets on measles and whooping cough (Duncan et al. 1996; Rohani et al. 1999). Recently, a transient relationship between cholera prevalence and El Niño oscillations in Bangladesh has been identified (Rodó et al. 2002).

Wavelet analysis overcomes the problems of non-stationarity in time series by performing a local time-scale decomposition of the signal, i.e., the estimation of its spectral characteristics as a function of time (Lau et al. 1995; Torrence and Campo 1998). Through this approach one can track how the different scales related to the periodic components of the signal change over time. Wavelet cross-spectrum and wavelet coherency generalize these methods, allowing the analyses of dependencies between two signals. It is worth noting that modified correlation approaches have also been proposed to account for the non-stationary nature of ecological time series (Rodriguez-Arias and Rodó 2004).

The potential of wavelet analysis appears particularly attractive given the specific nature of ecological and environmental time series and the relationships between them. In 2001, synchrony patterns of measles in the UK were revealed by wavelet analysis by Grenfell et al. (2001). They used wavelets to show a progressive increase in epidemic phase with time, accompanying the increasing trend in vaccination rates. Since this work, several applications of wavelet analysis have been published. Some of these papers were based on the characterization of time series and the analysis of their possible association with environmental signals. Nezlin and Li (2003) used wavelets to qualitatively compare the features of chlorophyll and environmental time series. Klvana et al. (2004) used wavelets to demonstrate the association between North American porcupine dynamics, local climate, and the solar cycle. Recent studies used wavelets to indicate an abrupt shift in the cyclic dynamics of Antarctic seabirds (Jenouvrier et al. 2005) and in Japanese vole dynamics (Saitoh et al. 2006). Cazelles et al. (2005) also used this approach to demonstrate a highly significant but non-stationary association between El Niño, precipitation and dengue epidemics in Thailand. Using similar approaches, Ménard et al. (2007) quantified the non-stationary association between climate and tuna populations in the Indian Ocean. Other papers have used the wavelet approach to compare the frequency features of simulated and observed data (e.g., Koelle and Pascual 2004) or to compare different analysis techniques (e.g., José and Bishop 2003, Rodriguez-Arias and Rodó 2004). Some analyses dealing with population synchrony use wavelets to extract the phase of the time series and to estimate phase synchrony (Rohani et al. 2003; Xia et al. 2004; Johnson et al. 2006). Wavelet analysis was also applied to the analysis of spatial patterns in vegetation systems (e.g., Bradshaw and Spies 1992; Dale and Mah 1998; Rosenberg 2004; Keitt and Urband 2005; Mi et al. 2005). Despite the fact that most papers deal with discrete wavelet transforms (DWT), Mi et al. (2005) offer an interesting comparison of results obtained using different continuous wavelet functions for an analysis of ecological patterns. Nevertheless the analyses of spatial patterns appear quite different to those of ecological time series, which are the focus of this paper.

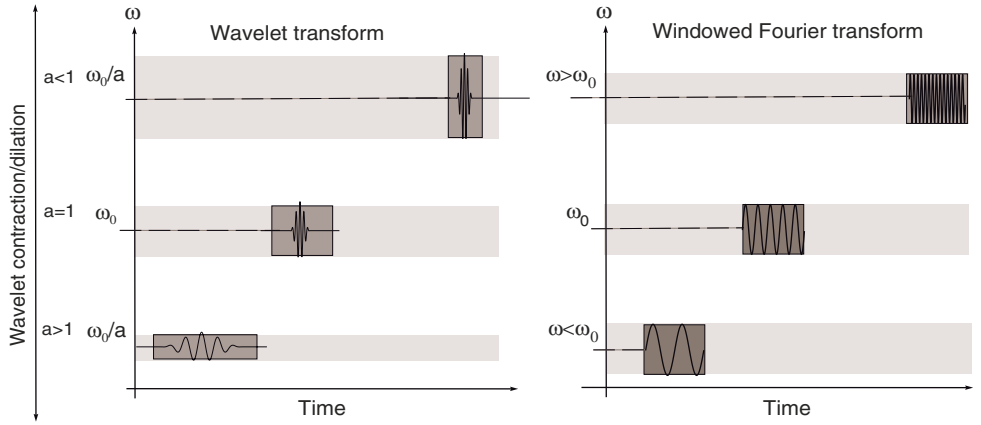

Fig. 1 Time–frequency resolution of the wavelet approach. *Left-hand panel* Examples of wavelets and their time–frequency boxes representing the corresponding variance distribution. When the scale (a) decreases, the time resolution improves but the frequency resolution becomes poorer and is shifted towards high frequencies. Conversely, if a increases, the boxes shift toward the region of low frequencies and the height of the boxes decreases (with a better frequency resolution) but they become wider (with a poor time resolution). *Right-hand panel* In contrast to wavelets, all the boxes of the windowed Fourier transform are obtained by a time or frequency shift of a unique function, which yields the same variance spread over the entire time–frequency plane

In the following, we present the basic ideas of the wavelet analysis for time-series analysis and its key features illustrated by both synthetic and ecological examples. Our main goal is to emphasize the advantages of this technique in the context of time-series analyses in ecology and population biology. It is worth noting that most of the studies that used wavelets in population dynamics only dealt with uni-variate time series. Here, we show that wavelet approaches are also of interest for the analyses of bi-variate time series.

Theory: the wavelet analysis

Although Fourier analysis is well suited to the quantification of constant periodic components in a time series, it cannot characterize signals whose frequency content changes with time. Whereas a Fourier decomposition may determine all the spectral components embedded in a signal, it does not provide any information about when they are present. To overcome this problem, several solutions have been developed in the past decades which are more or less able to represent a signal in the time and frequency domain at the same time. The aim of these approaches is to expand a signal into different waveforms with local time–frequency properties well adapted to the signal's structure. Gabor (1946) introduced a windowed Fourier decomposition to quantify the time–frequency content of signals. This short-time or windowed Fourier transform provides a decomposition of the signal in a time–frequency plane whose partition is layered by rectangular cells of the same size (Fig. 1). The time–frequency localization of this approach is, however, inefficient because the frequency resolution is the same for all the frequencies. A transient (with higher frequencies) needs a high time resolution to be well localized in time (Fig. 1). In contrast, a low-frequency structure might need a small time resolution (Fig. 1).

The wavelet transform decomposes a signal over functions (wavelets) that are narrow when high frequency features are focused and wide on low frequency structures (Daubechies 1992; Lau and Weng 1995). This decomposition leads to a good trade-off for the time-scale resolution, which is related to frequency resolution. This also allows a good localization in both time and frequency (Fig. 1), which is well suited to investigations of the temporal evolution of aperiodic and transient signals. Indeed, wavelet analysis is the time–frequency decomposition with the optimal trade-off between time and frequency resolution (Lau and Weng 1995; Mallat 1998).

Continuous wavelet approach

The wavelet transform decomposes signals over dilated and translated functions called "mother wavelets" $\varphi(t)$ that can be expressed as the function of two parameters, one for the time position (τ), and the other for the scale of the wavelets (a). More explicitly, wavelets are defined as $\varphi_{a,\tau}(t) = \frac{1}{\sqrt{a}}\varphi\left(\frac{t-\tau}{a}\right)$. The wavelet transform of a time series $x(t)$ with respect to a chosen mother wavelet is performed as follow:

$$W_x(a,\tau) = \frac{1}{\sqrt{a}}\int_{-\infty}^{+\infty} x(t)\varphi^*\left(\frac{t-\tau}{a}\right)dt = \int_{-\infty}^{+\infty} x(t)\varphi^*_{a,\tau}(t)dt \quad (1)$$

where * denotes the complex conjugate form. The wavelet coefficients, $W_x(a,\tau)$, represent the contribution of the scales

(the a values) to the signal at different time positions (the τ values). The wavelet transform can be thought as a cross-correlation of a signal $x(t)$ with a set of wavelets of various "widths" or "scales" a, at different time positions τ.

Figure 2 attempts to visualize the signification of the wavelet transform. In Fig. 2d a mother wavelet of scale a centered at location τ is shown superimposed on an arbitrary time series. In the case of good matching between the signal (x) and the wavelet (φ), the integral of the product of the signal with the wavelet of scale a produces a large positive value for the real part of wavelet transform, $\Re(W_x(a,\tau))$, at the position τ (Fig. 2d). When the matching is low, $\Re(W_x(a,\tau))$ takes low values. But an association in the opposite phase results in a high negative value for the real part of wavelet transform (Fig. 2d). By moving the wavelet along the signal (by increasing the τ parameter), structures relating to a specific scale a can be identified. This process is repeated over continuous ranges of a and τ to identify all the coherent structures within the signal (Fig. 2e). This produces a two-dimensional surface of $\Re(W_x(a,\tau))$ (Fig. 2e).

Note that the choice of the wavelet function $\varphi(t)$ is not arbitrary. This function is normalized to have unitary variance $\left(\int|\varphi(t)|^2dt=1\right)$ and it verifies $\int\varphi(t)dt = 0$. The wavelet decomposition is therefore a linear representation of the signal where the variance is preserved (Daubechies 1992). This implies that the original signal can be recovered by means of the inverse wavelet transform:

$$x(t)=\frac{1}{C_g}\int_{-\infty}^{+\infty}\int_{0}^{\infty}\frac{1}{a^2}W_x(a,\tau)\varphi_{a,\tau}(t)d\tau da \qquad (2)$$

where $C_g=\int_0^\infty\frac{\|\hat{\varphi}(f)\|^2}{f}df$ and $\hat{\varphi}(f)$ denotes the Fourier transform of $\varphi(t)$.

The wavelet transform is basically a linear filter whose response function is given by the wavelet function. By means of the inverse transform, the original signal can be recovered by integrating over all scales and locations, a

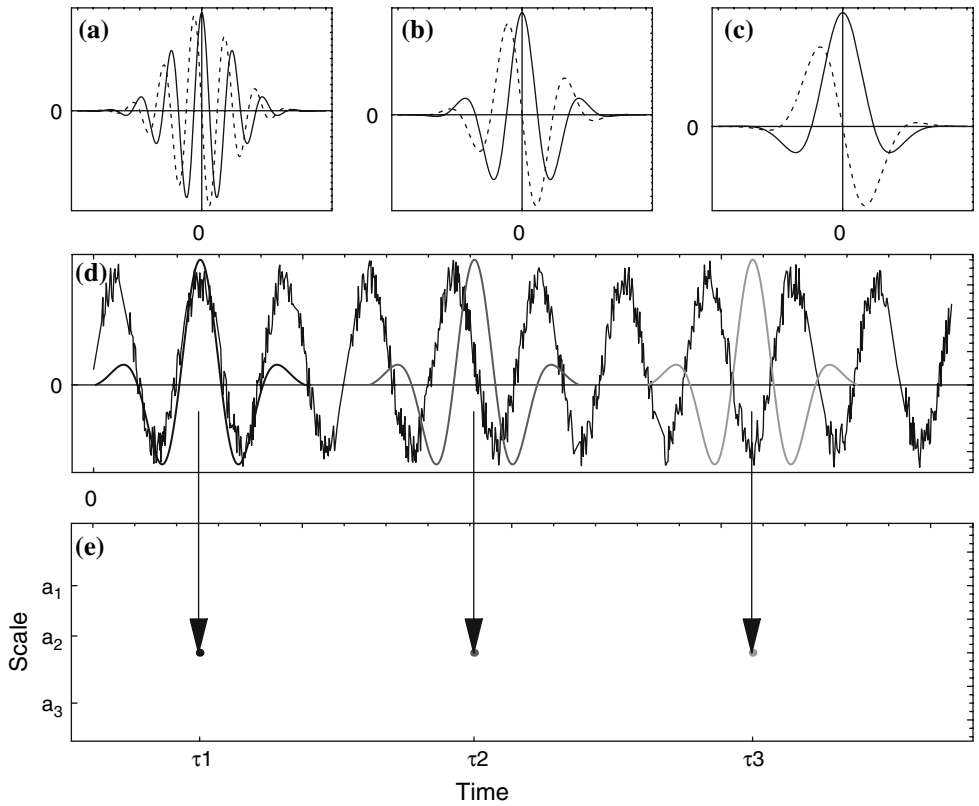

Fig. 2 Wavelet analysis. **a–c** Form of the Morlet wavelet as a function of the scale parameter a for $\tau = 0$: $a = a_1 = 0.5$ (**a**), $a = a_2 = 2$ (**b**), $a = a_3 = 4$ (**c**). Graphs display both the real part (*solid line*) and the imaginary part (*dashed line*) of the wavelet. **d** Morlet wavelet with $a = a_2$ is superimposed on a given signal at different time positions (τ_1, τ_2,τ_3). In τ_1, the matching between the signal and the wavelet is height; this will give a high positive value of the real part of the wavelet transform, $\Re(W_x(a,\tau_1))$. In τ_2, the matching is weak and the value of $\Re(W_x(a,\tau_2))$ will be low. Finally in τ_3, the signal and the Morlet wavelet are in a perfect opposite phase with similar period, and there will be a high negative value for $\Re(W_x(a,\tau_3))$. **e** Wavelet transforms [or quantities derived from $W_x(a,\tau)$] are plotted on a two-dimensional (2D) graph. As an example, **e** shows the value of $|W_x(a,\tau)|^2$ for $a = a_2$ and for the three time positions τ_1, τ_2 and τ_3 defined in **d**. The complete 2D plot is obtained simply by computing wavelet transforms for a given range of a and τ values

and τ. Nevertheless, one can limit the integration over a chosen range of scales, a_1–a_2, to perform a band-pass filtering of the original time series in this chosen range of scales.

Choice of the mother wavelet

There are several considerations in making the choice of a wavelet, for example, real versus complex wavelets, continuous or discrete wavelets, orthogonal versus redundant decompositions. Briefly, the continuous wavelets often yield a redundant decomposition (the information extracted from a given scale band slightly overlaps that extracted from neighboring scales) but they are more robust to noise as compared with other decomposition schemes. Discrete wavelets have the advantage of fast implementation but generally the number of scales and the time invariant property (a filter is time invariant if shifting the input in time correspondingly shifts the output) strongly depend on the data length. If quantitative information about phase interactions between two time series is required, continuous and complex wavelets provide the best choice (further details can be found in Mallat 1998). However, all the wavelets share a general feature: low oscillations have good frequency and poor time resolution whereas fast oscillations have good time resolution but a lower frequency resolution.

Two popular continuous wavelets are the "Mexican hat" and the "Morlet wavelet". The choice of the continuous wavelet can influence the time and the scale resolution of the decomposition (this decomposition is related to the frequency decomposition as seen below). Thus, as the Morlet wavelet is very well localized in scales and then in frequencies, a high frequency resolution is expected. In contrast, the Mexican hat wavelet has a good time localization (it can isolate a single bump), but a poor frequency localization. Mi et al. (2005) compared the results of the analysis of spatial pattern with the Mexican hat and the Morlet wavelets in an ecological context. They came to similar conclusions concerning the features of these wavelets. In our applications we have chosen the Morlet wavelet $\varphi(t) = \pi^{-1/4}\exp(-i2\pi f_0 t)\exp(-t^2/2)$, (Fig. 2a–c).

For some particular mother wavelets, the relation between the frequency and the wavelet scale can be derived analytically (e.g., Meyers et al. 1993). For the Morlet wavelet this equivalence is done by $\frac{1}{f} = \frac{4\pi a}{\omega_0 + \sqrt{2+\omega_0^2}}$, with ω_0 the central angular frequency of the wavelet ($\omega_0 = 2\pi f_0$). Then with ω_0 around 2π, the wavelet scale a is therefore inversely proportional to the central frequency of the wavelet, $f \approx {}^1/_a$. This greatly simplifies the interpretation of the wavelet analysis and one can replace, in all equations, the scale a by the frequency f or the period $p = 1/f$.

The Morlet wavelet has the advantage of having both real and imaginary parts. This allows separation of the phase and the amplitude of the studied signal. As $W_x(f,\tau)$ is a complex number, we can write $W_x(f,\tau)$ in terms of its phase $\phi_x(f,\tau)$ and modulus $|W_x(f,\tau)|$. The phase of the Morlet transform varies cyclically between $-\pi$ and π over the duration of the component waveforms and is defined as:

$$\phi_x(f,\tau) = \tan^{-1}\frac{\Im(W_x(f,\tau))}{\Re(W_x(f,\tau))} \tag{3}$$

Wavelet power spectrum

In one sense, the wavelet transform can be regarded as a generalization of the Fourier transform, and by analogy with spectral approaches one can compute the "local wavelet power spectrum" by $S_x(f,\tau) = \|W_x(f,\tau)\|^2$. The Fourier spectrum of a signal can be compared with the global wavelet power spectrum which is defined as the averaged variance contained in all wavelet coefficients of the same frequency f:

$$\overline{S_x}(f) = \frac{\sigma_x^2}{T}\int_0^T \|W_x(f,\tau)\|^2 d\tau \tag{4}$$

with σ_x^2 the variance of the time series x and T the duration of the time series. Another interesting computation is the mean variance at each time location, obtained by averaging the frequency components:

$$\overline{s_x}(\tau) = \frac{\sigma_x^2 \pi^{1/4}\tau^{1/2}}{C_g}\int_0^\infty \left(\frac{1}{f}\right)^{1/2} \|W_x(f,\tau)\|^2 df \tag{5}$$

This quantity can also be filtered in a given frequency band, f_1–f_2.

Wavelet coherency and phase difference

In many applications, it is desirable to quantify statistical relationships between two non-stationary signals. In Fourier analysis, the coherency is used to determine the association between two signals, $x(t)$ and $y(t)$. The coherence function is a direct measure of the correlation between the spectra of two time series (Chatfield 1989). To quantify the relationships between two non-stationary signals, the following quantities can be computed: the "wavelet cross-spectrum" and the "wavelet coherence".

The wavelet cross-spectrum is given by $W_{x,y}(f,\tau) = W_x(f,\tau)W_y^*(f,\tau)$,with * denoting the complex conjugate. As in the Fourier spectral approaches, the wavelet coherency is defined as the cross-spectrum normalized by the spectrum of each signal:

$$R_{x,y}(f,\tau) = \frac{\left\|\left\langle W_{x,y}(f,\tau)\right\rangle\right\|}{\left\|\left\langle W_{x,x}(f,\tau)\right\rangle\right\|^{1/2}\left\|\left\langle W_{y,y}(f,\tau)\right\rangle\right\|^{1/2}} \quad (6)$$

where '$\langle\rangle$' denotes a smoothing operator in both time and scale. Using this definition, $R_{x,y}(f,\tau)$ is bounded by $0 \leqslant R_{x,y}(f,\tau) \leqslant 1$. The smoothing is performed, as in Fourier spectral approaches, by a convolution with a constant-length window function both in the time and frequency directions (Chatfield 1989).

The advantage of these "wavelet-based quantities" is that they vary in time, and can, therefore, detect transient association between studied signals (Liu 1994). These quantities provide local information about where the two non-stationary time series are linearly correlated at a particular frequency (or frequency band) and temporal location in the time–frequency plane. They can also be interpreted as the fractional portion of power of $x(t)$ that is in common (i.e., it can be accounted for by a linear relationship) with that of $y(t)$ at a particular time and frequency band. The wavelet coherence $R_{x,y}(f,\tau)$ is equal to 1 when there is a perfect linear relation at particular time location and frequency between the two signals.

To obtain information about the possible delay in the relationship (i.e., in phase or out of phase relations), with complex wavelets one has the opportunity to compute the phase difference $\phi_{x,y}(f,\tau)$ and possibly the distribution of phase difference. The phase difference reads:

$$\phi_{x,y}(f,\tau) = \tan^{-1}\frac{\Im(\langle W_{x,y}(f,\tau)\rangle)}{\Re(\langle W_{x,y}(f,\tau)\rangle)} \quad (7)$$

A unimodal distribution of the phase difference (for the chosen range of scales or periods) indicates there is a preferred value of $\phi_{x,y}(f,\tau)$ and thus a statistical tendency for the two time series to be phase locked. Conversely, the lack of association between the phase of $x(t)$ and $y(t)$ is characterized by a broad and uniform distribution. To quantify the spread of the phase difference distribution one can use circular statistics or quantities derived from the Shannon entropy (Pikovsky et al. 2001; Cazelles and Stone 2003).

Zero padding and the cone of influence

In practice, the wavelet power spectrum is computed by first taking a discrete Fourier transform of the time series. For each scale, the wavelet's frequency response is then analytically computed and it is multiplied by the data's transform in the frequency domain. The Fourier inverse transform of this product is finally taken. This, however, requires certain periodicity assumptions in both the data and the response function of the wavelet. In order to avoid false periodic events ("wrap-around" artifacts), zero padding is needed. Currently, the length of the time series is artificially increased, to the next-higher power of two, by adding zero-value samples. Nevertheless, the disadvantage of zero padding is that discontinuities are artificially created at the border of the data. As the wavelet gets closer to the edge of the time series, part of it exceeds the edge and thus the values of the wavelet transform are affected (reduced) by the zeros introduced creating the boundary effect. Further, the affected region increases in extent as the scale a (or the frequency f) of the wavelet increases. This zone where edge effects are present, is called the "cone of influence" (see Torrence and Campo 1998) and the spectral information below the cone is lacking in accuracy and should be interpreted with caution.

Assessment of statistical significance

As with other time-series methods, it is crucial to assess the statistical significance of the patterns exhibited by the wavelet approach. To this end, we suggest employing bootstrapping methods. The idea is to construct, from observed time series, control data sets, which share some properties with the original series but are constructed under a defined null hypothesis. There exists a large range of null hypotheses and associated re-sampling procedures ranging from simple bootstrap (Efron and Tibshirani 1993) to more complex resampling that preserves the autocorrelation function of the raw time series (see Theiler et al. 1992). It is clear that a simple random shuffling of data generates a white noise process that appears as a "weak" null-hypothesis that should be rejected easily. At the other extreme, the surrogate by Theiler et al. (1992) mirrors a "hard" null-hypothesis that should be rejected with difficulty in the case of wavelet analysis because these bootstrapped series and the raw series share the same autocorrelation function (see Rouyer et al. 2008). Here, we have chosen to use a procedure based on a resampling of the observed data with a Markov process scheme that preserves only the short temporal correlations (see Cazelles and Stone 2003). Our aim is to test whether the wavelet-based quantities (e.g., the spectra or coherence) observed at a particular position on the time-scale plane are not due to a random process with the same Markov transitions (time order) as the original time series. Technically the bootstrapped series are computed in the following way:

1. The time series $\{x_i\}$ (or $\{y_t\}$) is binned to form a frequency histogram of n_h equal-sized bins.
2. A transition matrix M that describes the time evolution from bin-i to bin-j is then estimated based on the actual relative frequencies of the data contained within bin-i, $M_{ij} = \Pr\left(x_{n+1} \in b_j | x_n \in b_i\right)$.
3. To construct a bootstrapped time series $\{z_i\}$, an initial value z_0 is randomly chosen from the raw series.

4. To determine z_{n+1} having obtained already z_n the probability M_{ij} that z_n from bin b_i ends up in bin b_j is used. With M_{ij} the bin b_j associated with z_{n+1} is randomly chosen. z_{n+1} is then computed by making a random selection from the elements in bin b_j.
5. The last step is iterated to obtain a surrogate series of the same length as the raw series.

For each bootstrapped series the wavelet transform and "related quantities" are computed. As the process is repeated n_b times, the distribution of these "wavelet quantities" under the null hypothesis is constructed. We can compare the wavelet quantities of the raw series with their distribution under the null hypothesis, extracting, for instance, the 99th or the 95th percentiles of this distribution. It is important to note that we also used other null hypotheses and associated resampling schemes (e.g., simple bootstrapping, white noise, red noise) and similar conclusions were reached. A possible explanation of this weak sensitivity of the choice of the resampling scheme to our results may be related to key features of the analyzed time series that are short and noisy. The results from the statistical tests may mainly be affected by the breakdown of the time order of the time series.

From theory to practice: analysis of non-stationary synthetic time series

Synthetic signals with identical power spectrum

The main property of the wavelet approach is to introduce the possibility of identifying a time–frequency discrepancy of studied signals. This allows one to distinguish between two signals that have identical periodic components and a similar power spectrum.

We have used two signals composed of two periodic components of period (p_1 and p_2). For the first signal, the two periodic components are present during the whole interval of observation:

$$y(t) = \mu + \frac{1}{2}\sin\left(\frac{2\pi t}{p_1}\right) + \frac{1}{2}\sin\left(\frac{2\pi t}{p_2}\right) + \varepsilon \tag{8}$$

where μ is the mean of the time series, p_1 and p_2 are the two periods and ε is a Gaussian noise component with a weak variance. For the second, the two periods are temporally localized on the first and the second half-part of the time series:

$$\begin{aligned} y(t) &= \mu + \sin\left(\frac{2\pi t}{p_1}\right) + \varepsilon \quad \text{if} \quad t < t_s \\ y(t) &= \mu + \sin\left(\frac{2\pi t}{p_2}\right) + \varepsilon \quad \text{if} \quad t \geqslant t_s \end{aligned} \tag{9}$$

where t_s is the time of the shift of the periodicity of the signals.

These two time series are displayed in Fig. 3a, c. For their analyses 200 data points have been used. Despite their large discrepancy (Fig. 3a, c), these two signals have quasi identical power spectrum (Fig. 3b, d) with the same two distinct peaks at the significant periods p_1 and p_2. Contrary to the Fourier spectrum, with wavelet analysis one can clearly discriminate the temporal difference of these two signals (Fig. 3e, g). Based on these figures, one can easily observe that in the first case the two periodic components are present during the whole time series (Fig. 3e), whereas in the second the period of the time series shifts from p_1 to p_2 at time $t_s = 5$ (Fig. 3g). For the first signal (Eq. 8) the dominant periodic components appear as a horizontal band centered at the two periodic components, reflecting the constancy of these periodic components in time. For the second (Eq. 9) one can observe that only one component is present for the two half-parts of the series with a discontinuity in the period of this component around time $t_s = 5$. We have also plotted the average wavelet power spectrum (Fig. 3f, h) to allow the reader to see the correspondence between the continuous wavelet approaches and Fourier spectral analysis (Fig. 3b, d).

A synthetic signal with transient periodic and amplitude components

Here, we examine the wavelet signature of gradual or abrupt changes in the amplitude or frequency of a simple sinusoidal signal. This sinusoidal model reads:

$$\begin{aligned} y(t) &= \mu + A_1 \sin\left(\frac{2\pi t}{p_2}\right) + \varepsilon \quad \text{if} \quad t < t_{s1} \\ y(t) &= \mu + A_2 \sin\left(\frac{2\pi t}{p_1}\right) + \varepsilon \quad \text{if} \quad t_{s1} < t < t_{s2} \\ y(t) &= \mu + A(t) \sin\left(\frac{2\pi t}{p(t)}\right) + \varepsilon \quad \text{if} \quad t \geq t_{s2} \end{aligned} \tag{10}$$

with $A(t) = A_2 + (A_1 - A_2)\frac{t-t_{s1}}{t_{s2}-t_{s1}}$, $p(t) = p_1 + (p_2 - p_1)\frac{t-t_{s1}}{t_{s2}-t_{s1}}$, $A_1 = 2$, $A_2 = 1, \varepsilon$ is a small Gaussian perturbation and t_{si} are the time shifts of the features of the time series.

This signal with 200 data points is displayed in Fig. 4a. The Fourier spectrum summarizes the average characteristic of this signal and identifies a broad period around 1 unit of time (u.t.) (Fig. 4b). Using wavelet analysis one can reconstruct the time evolution of the main oscillating components of the time series. Figure 4c shows the wavelet transform of the signal, where wavelets of different time-offsets and frequencies resonate with the signal at different time points. Based on the wavelet power spectrum (Fig. 4d), one can easily observe that in the first part of the time series the dominant period is around $p_2 = 1$ u.t., then at t_{s1} this period shifts to $p_1 = 0.25$ u.t. and it increases from $p_1 = 0.25$ to $p_2 = 1$ u.t. after t_{s2}. Figure 4e shows how the time-averaged wavelet power spectrum is very similar to the Fourier spectrum (Fig. 4b). With wavelet

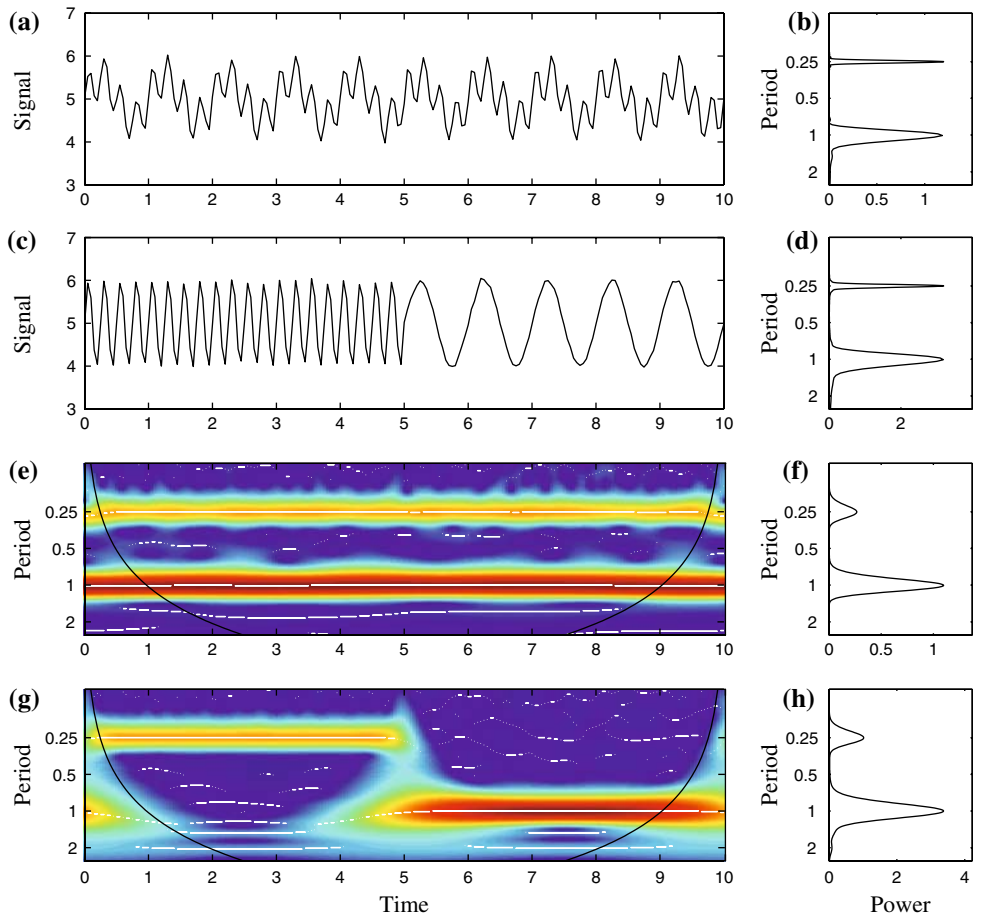

Fig. 3 Wavelet analysis of sinusoidal signals with two periodic components. **a** A signal with a periodic component present during the whole series [$\mu = 5$, $p_1 = 0.25$ unit of time (u.t.) and $p_2 = 1$ u.t.]. **b** Fourier spectrum of the signals displayed in **a**. The periodograms have been smoothed with a Parzen window (Chatfield 1989). **c** A series with the same periodic components as those of **a** but these two periodic components are localized on the first and on the second half-part of the signal, the period shift is at $t_s = 5$. **d** Fourier spectrum of the signals displayed in **c**. **e** Wavelet power spectrum of the signal displayed in **a**. The colors code for power values from *dark blue* (low values), to *dark red* (high values). *Dotted white lines* materialize the maxima of the undulations of the wavelet power spectrum and the *black line* indicates the cone of influence that delimits the region not influenced by edge effects. **f** Average wavelet power spectrum $(\overline{S_x}(f))$ of the signal in **a**. **g**, **h** As in **e**, **f** but for the signal displayed in **c**

decomposition one has also the possibility to examine fluctuations of the variance of the time series over both time and a range of period. Figure 4e shows this evolution for the sinusoidal signal over different bands. One can easily observe the dominance of the 0.25 u.t. periodic component between t_{s1} and t_{s2} and of 1 u.t., before t_{s1} and after t_{s2}.

In this example, whereas the Fourier spectrum was not able to differentiate temporally between the different periodic components, the wavelet analysis clearly identifies both the abrupt periodic shift at $t_{s1} = 3$ and the smooth increase of the period after $t_{s2} = 5.25$.

Influence of the number of data points and observational noise

To stress the robustness of the wavelet approach for ecological applications, we focus on the effect of the number of data points used for the analysis and also on the potential effect of the observational noise.

We use a lag-2 autoregressive [AR(2)] model with two parameter sets in a reasonable ecological range (Royama 1992), as an illustrative example of non-stationary dynamics. The model reads:

$$\begin{aligned} y(t) &= a_1 + b_1 y(t-1) + c_1 y(t-2) + \varepsilon_1 \quad \text{if} \quad t < t_s \\ y(t) &= a_2 + b_2 y(t-1) + c_2 y(t-2) + \varepsilon_2 \quad \text{if} \quad t \geq t_s \end{aligned} \tag{11}$$

where a_i, b_i and c_i are the parameters of the autoregressive model and ε_i are the noise perturbations which are Gaussian with variance σ_i^2. The two sets of parameters are chosen to obtain dynamics with two different main periodicities before and after t_s. Figure 5a shows the analyzed time series with $n = 100$ data points and Fig. 5b shows the wavelet power spectrum. One can observe the abrupt

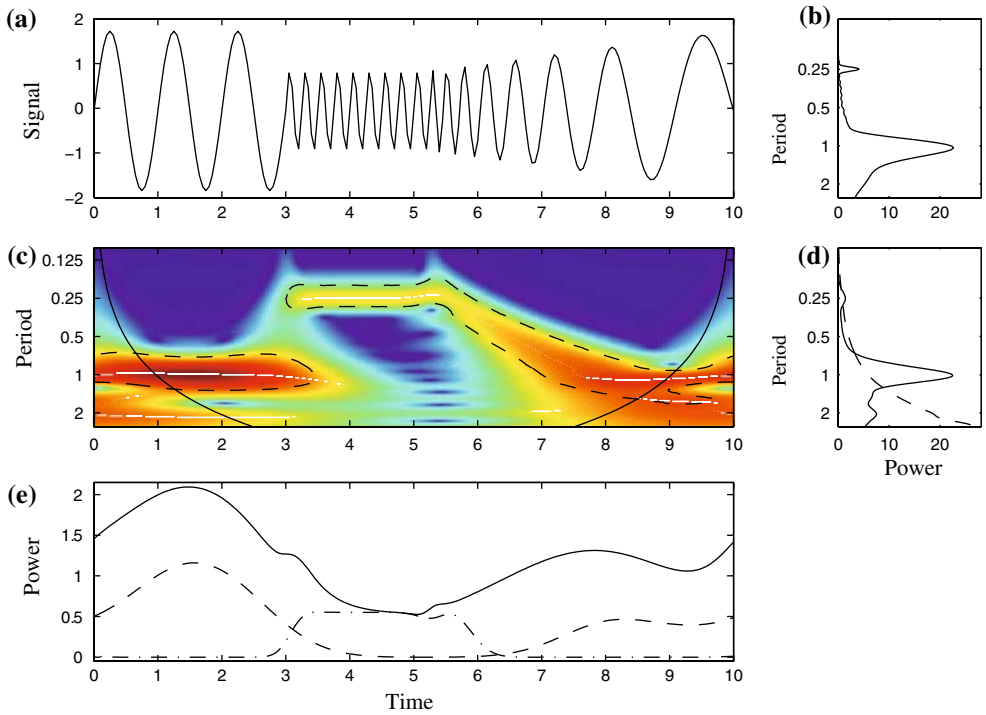

Fig. 4 Synthetic transient signal studied with wavelet approach. **a** A transient time series with modification of both the amplitude and the period described by Eq. 10 with $\mu = 5$, $t_{s1} = 3$ and $t_{s2} = 5.25$. **b** Fourier spectrum of the signal displayed in **a**. The periodogram has been smoothed with a Parzen window (Chatfield 1989). **c** Wavelet power spectrum of the signal. The colors code for power values from *dark blue* (low values) to *dark red* (high values). *Dotted white lines* materialize the maxima of the undulations of the wavelet power spectrum and the *black line* indicates the cone of influence that delimits the region not influenced by edge effects. **d** Average wavelet power spectrum $(\overline{S_x}(f))$ of the signal. On the graphs **c**, **d** *dashed lines* show the $\alpha = 5\%$ significance levels computed based on 1,000 Markov bootstrapped series. **c** *P*-values associated with the values within the area delineated by the *dashed line* are less than 5%. **e** Frequency-average wavelet power for the signal displayed in **a**, over the 0.1–5 u.t. band (*black line*), around the 1 u.t. band (*dashed line*) and around the 0.25 u.t. band (*dotted–dashed line*)

variation of the main periodicity around $t_s = 60$. The period is ca. eight iterations before t_s, and ca. four iterations after. These two periodic components also appear clearly on the average wavelet power spectrum (Fig. 5c). What appears to be particularly interesting is that these results can also be found with just half of the data points (Fig. 5d–g). Of course, when halving the number of data points, some information is lost and the periodicity appears less obvious, but similar conclusions can be drawn (Fig. 5d–g).

Another interesting result relates to the robustness of the results when observational noise is added to the time series. Figure 5h–i shows results of analyses performed only on the even data points of the time series when Gaussian observational noise with a variance proportional to the variance of the complete time series is added. Even with this noisy and short signal, results do not differ from those obtained with the raw series.

These simulations have been repeated ($k = 100$) and the two significant periodic bands around eight iterations before $t_s = 60$ and around four iterations after *ts* were present each time. Moreover, based on classic ANOVA, the differences between the k average P-values in the significant periodic bands appear non-significant.

Relationships between two synthetic signals

To illustrate the possibility of quantifying an association between two time series, we used two AR(2) models with slightly different parameter values but with correlated noise components. The two series were correlated even when they had slightly different oscillating components, since the noise components were correlated. This is known as the "Moran effect" (see Royama 1992).

A weak correlation between the noise components ($\rho_{\varepsilon_x,\varepsilon_y} = 0.50$) was used. The correlation between the series was thus also weak. Figure 6 summarizes the results of the wavelet analysis (the normalized time series, the wavelet cross-spectrum, its average, and the wavelet coherency are shown in Fig. 6a–d, respectively). The main co-variance between the two time series is in the 7–9 period band (Figs 6b, c). The association between the two time series (quantified as the coherence) is significant in the same

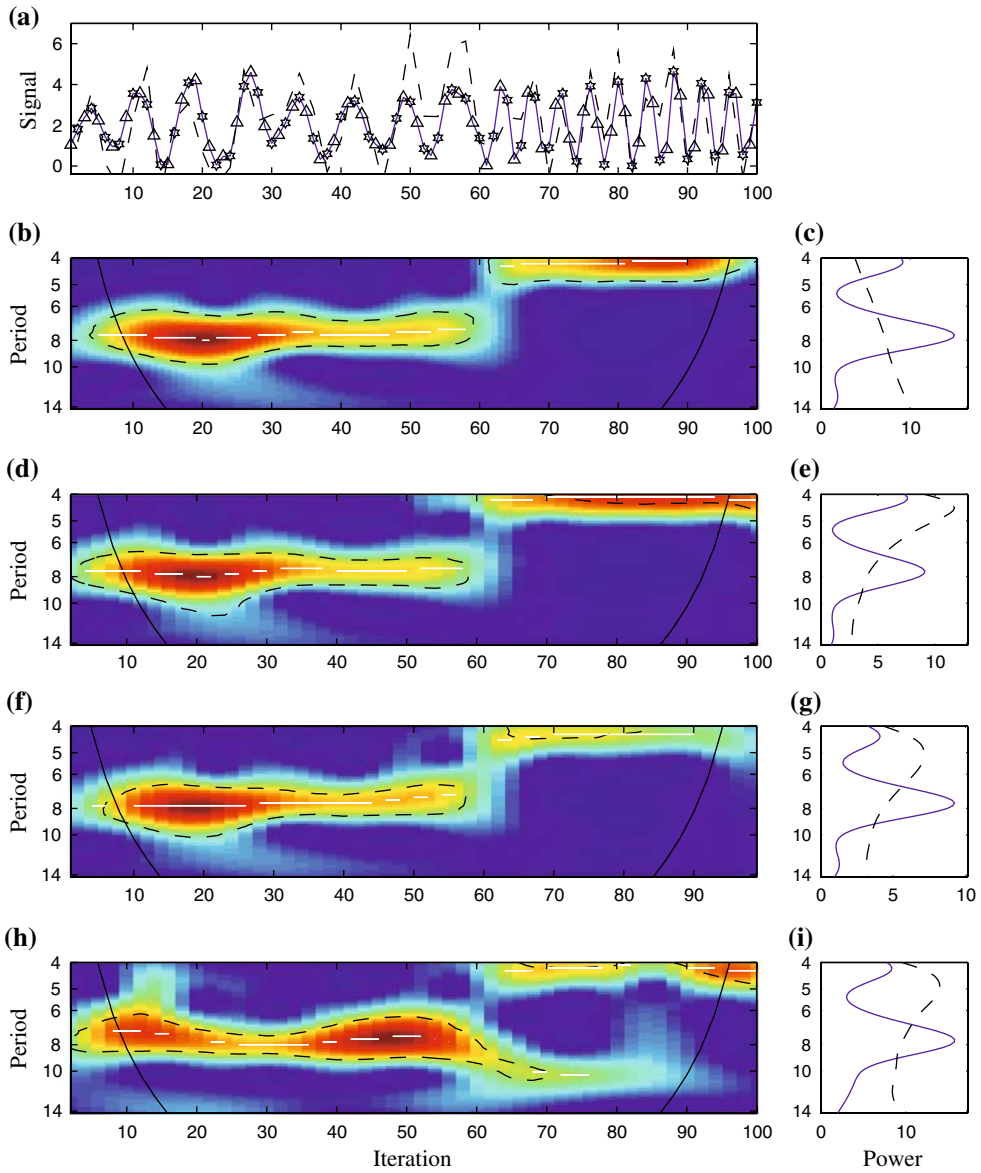

Fig. 5 Influence of the number of data point and the observational noise on wavelet analysis. **a** The time series is generated with the lag-2 autoregressive [AR(2)] models (Eq. 11). *Triangles* indicate the odd data point, *stars* even data points and the *dashed line* noisy even data points. **b** Wavelet power spectrum of the full data set ($n = 100$ and the sampling time step $\Delta t = 1$). **d** Wavelet power spectrum of the odd data points ($n = 50$ and $\Delta t = 2$). **f** Wavelet power spectrum of the even data points ($n = 50$ and $\Delta t = 2$). **h** Wavelet power spectrum of the even data points ($n = 50$ and $\Delta t = 2$) when observational noise is added ($\sigma_i = 0.80\ \sigma_x$). **c–i** Average wavelet power spectrum corresponding to the wavelet power spectrum plotted in **b–h**, respectively. On the wavelet power spectrum graphs, the *dashed lines* show the $\alpha = 5\%$ significance levels computed based on 1,000 Markov bootstrapped series. On these 2-D graphs (**b–h**), the colors code for power values from *dark blue* (low values), to *dark red* (high values), the *dotted white lines* materialize the maxima of the undulations of the wavelet power spectrum, the *black lines* indicate the cone of influence that delimits the region not influenced by edge effects and the *P*-values associated with the values within the area delineated by the *dashed line* are less than 5%. The parameters used for the AR(2) models are: $a_1 = 1.5$, $b_1 = 1.2$, $c_1 = -0.9$, $\sigma_1^2 = 0.15$, $a_2 = 4$, $b_2 = 0.1$, $c_2 = -1$, $\sigma_2^2 = 0.05$ and $t_s = 60$

period band, but this association appears more discontinuous, with high coherence only between the iterations 1–20, 35–55 and 75–90 (Fig. 6e). There are also some significant areas for the 12–16 mode. To obtain information about the sign of the association and the possible delay in the relationship, we have computed the phases of the two signals for the 7–9 period band, as well as the phase difference (Fig. 6e). Results show that the two time series are out of phase with a short delay around $\pi/2$, except for the time interval 35–55 where the two series are in phase. Due to the transient behavior of the association between the series, the distribution of phase difference (Fig. 6f) appears

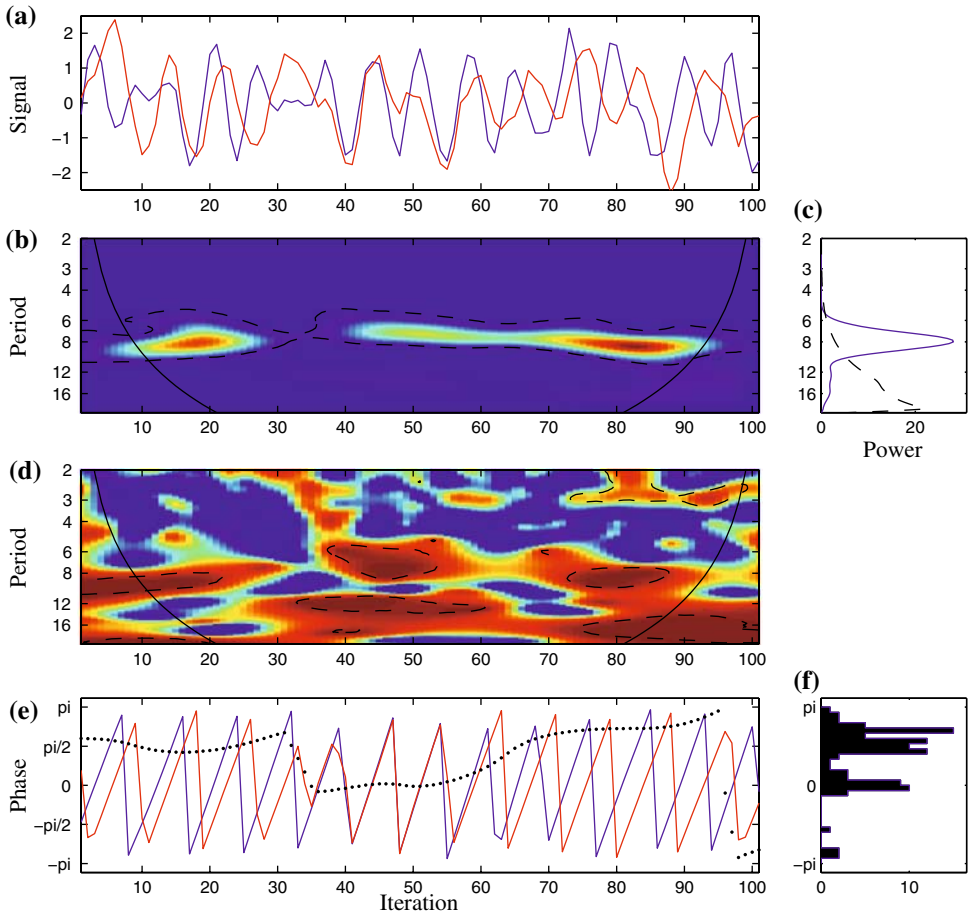

Fig. 6 Quantification of the association between two synthetic signals with the wavelet approach. **a** Time series, $x(t)$ and $y(t)$, generated with two different AR(2) models with correlated noise components (n = 100). These series have been normalized for the analyses. **b** Wavelet cross-spectrum. **c** Average wavelet cross-spectrum. **d** Coherence between the two time series. Colors code from *dark blue* (low values) to *dark red* (high values) and the *black lines* indicate the cone of influence that delimits the region not influenced by edge effects. On the graphs **b**–**d** *dashed lines* show the $\alpha = 5\%$ significance levels computed based on 1,000 Markov bootstrapped series. P-values associated with the values within the region delineated by the *dashed line* are less than 5%. **e** Phases of the two time series computed in the 7–9 periodic band; *dotted line* represents the phase difference. **f** Distribution of the phase difference of the two time series. The parameters used for the AR model are: $a_x = 1.5$, $b_x = 1.2$, $c_x = -0.9$, $\sigma_x^2 = 0.025$, $a_y = 1, b_y = 1.35$, $c_y = -0.75$, $\sigma_y^2 = 0.025$ and $\rho_{\epsilon_x,\epsilon_y} = 0.50$

bimodal, so that it is difficult to test the significance of this distribution in this particular case.

Real life data: analysis of ecological time series

Grouse dynamics as an example of transient periodic dynamics

Records of shooting bags in northeast Scotland (MacKenzie 1952) have generated long ecological time series representing fluctuations in red grouse populations (Fig. 7a). The Fourier spectrum of this series is dominated by high periods between 40 and 50 years (Fig. 7b). These periods correspond approximately to half the length of the time series, underlying some form of non-stationarity where the amplitude of variance of the series differs between the first and second parts of the series. After detrending the time series, which is the classic approach used for reducing non-stationarity (Chatfield 1989), one can observe a first peak around 3 years and a second broader peak between 5 and 6 years (Fig. 7d). Nevertheless, this classic approach may lead to a misleading interpretation of the dominant oscillating components and their time localization.

Wavelet analysis allowed us to decompose the grouse abundance variability from 1849 to 1945 as a function of period and time. Figure 7e shows the wavelet power spectrum for the grouse time series and Fig. 7f shows the average wavelet power spectrum (which appears similar to the Fourier spectrum, see Fig. 7c). Statistically significant periodicity is revealed, although only for some restricted period of time; for the 5–6 year mode from 1860 to 1875,

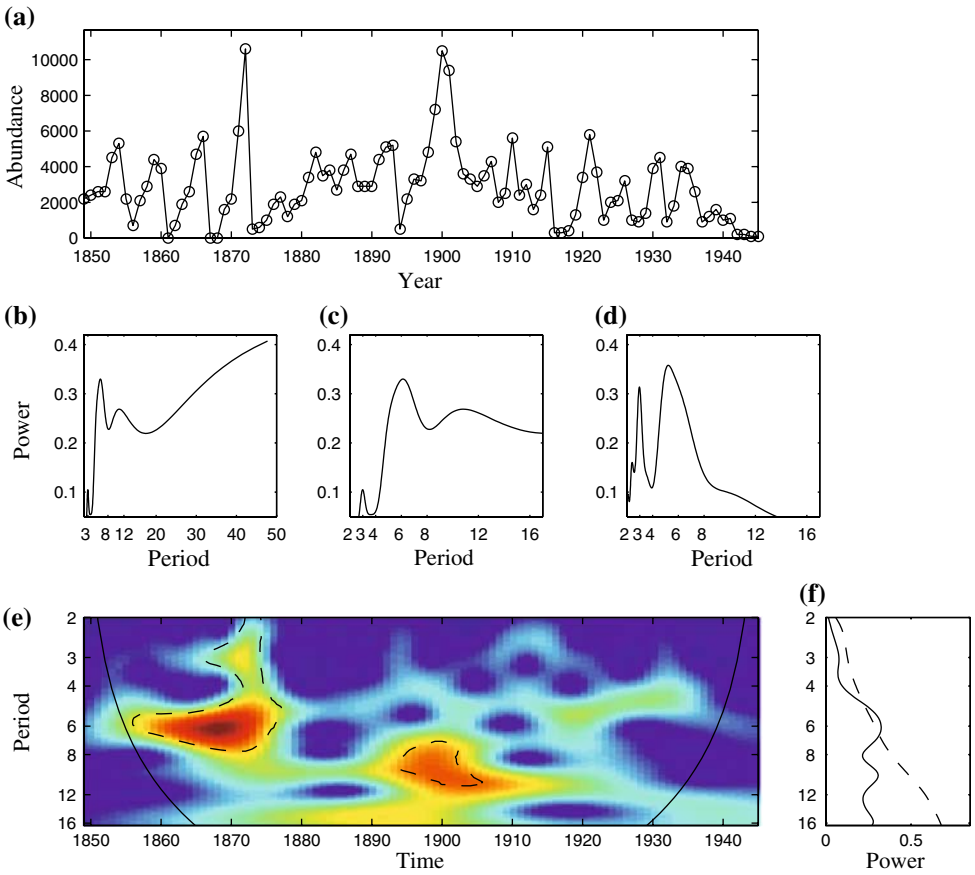

Fig. 7 A non-stationary ecological time series, the red grouse population in northeast Scotland (MacKenzie 1952). Grouse time series estimated based on records of shooting bags (97 data points). **b** Power spectrum of the raw time series. **c** Enlargement of **b**. **d** Power spectrum of the detrended time series. The periodograms have been smoothed with a Parzen window (Chatfield 1989). **e** Wavelet power spectrum, $|W_x(f,\tau)|^2$, of the grouse series. The colors code for power values from *dark blue* (low values) to *dark red* (high values) and the *black line* indicates the cone of influence that delimits the region not influenced by edge effects. **f** Average wavelet power spectrum of the grouse series. On the graphs **e**, **f** *dashed lines* show the $\alpha = 5\%$ significance levels computed based on 1,000 Markov bootstrapped series. *P*-values associated with the values within the region delineated by the *dashed line* are less than 5%

and for the 8–10 year mode from 1895 to 1910 (Fig. 7d). These results emphasize the non-stationary behavior of the grouse abundance and the absence of a single persistent mode of variability within the time interval 1849–1945.

Population fluctuations and the solar cycle

Several studies have suggested that the solar cycle could impact climate and then indirectly fluctuations of animal populations (Elton 1924; Royama 1992). This sunspot hypothesis was for example put forth to explain the 10-year lynx cycle in Canada (Sinclar et al. 1993), although the issue is still controversial. Recently, Klvana et al. (2004) have shown that porcupine abundance in eastern Quebec has fluctuated periodically since 1868. They have also demonstrated that these oscillations have a strong association with both the solar cycle and local climate fluctuations.

Here we show how wavelet analyses can contribute to the debate surrounding the possibility of a relationship between the 10-year solar cycle, climate and population fluctuations. We compare the association between the sunspot number and: (1) lynx population abundance, and (2) porcupine population abundance. The lynx time series analyzed is the series from the MacKenzie River region (Elton and Nicholson 1942) and the porcupine time series comes from a dendrochronological reconstruction of porcupine abundance (Klvana et al. 2004). As shown in Fig. 8b–d, the association between sunspot number and lynx abundance appears very weak and significant in the 10–12 periodic band only for the time periods 1821–1840 and 1915–1934. In addition, the phase analysis shows that for the time period 1821–1840 the two series are in phase while for 1915–1934 the two series are out of phase with a delay of $3\pi/2$ or 3/4 of the quasi-period (Fig. 8c). Conversely, we obtained a strong association between porcupine abundance and the sunspot number in the 10–12 periodic band for virtually the full length of the time series (Fig. 8e–g). This relation is weaker during 1940–1980 when the oscillations are coherent around the 22-year periodic band (Fig. 8e). The coherence is also very significant around the 22-year mode as stressed in Klvana et al. (2004). Phase analysis reveals (Fig. 8f) that the two series are out of phase with an approximate delay of half a quasi-cycle (π). The sign of the association is then negative. Furthermore, this relationship between the phases of the two series is highly significant (Fig. 8g).

Wavelet analyses allowed us to take into account the non-stationary nature of the associations between

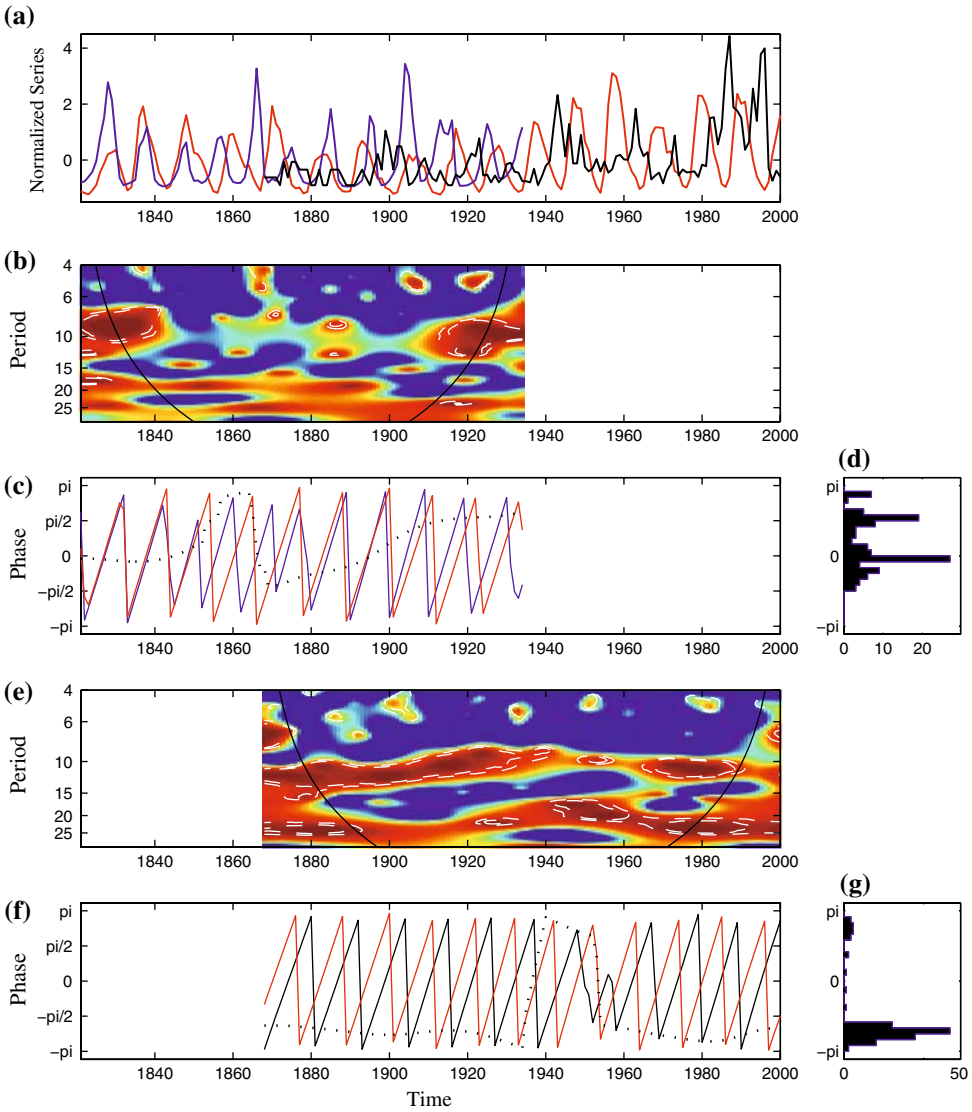

Fig. 8 Comparison between the association between the sunspot numbers and the lynx population and between the sunspot numbers and the porcupine population. **a** Normalized time series: the sunspot numbers (*red line*), the lynx abundance (*blue line*) and the porcupine abundance (*black line*). Note that the lynx and porcupine time series have a different starting date and different length, which explains the blank spaces in the following graphs. **b**–**d** Lynx-sunspot analyses and **e**–**g** porcupine-sunspot analyses. **b**, **e** Wavelet coherency between the population abundance and the sunspot numbers. Colors code for coherence values from *dark blue* (0) to *dark red* (1). *Black line* indicates the cone of influence that delimits the region not influenced by edge effects and *dashed lines* show the $\alpha = 5\%$ and $\alpha = 10\%$ significance levels computed based on 1,000 Markov bootstrapped series. **c**, **f** Phases of the population abundance and the sunspot numbers computed in the 10–12 year periodic band. *Dotted line* represents the phase difference and the colors are as in **a**. **d**, **g** Distribution of the phase difference of the two considered time series. **d** Normalized entropy of this phase difference distribution (see Cazelles and Stone 2003) is $Q = 0.19$ and it is not significant. **g** Normalized entropy of this distribution is $Q = 0.47$ and it is significant with a *P*-value computed with 1,000 Markov bootstrapped series less than 0.1%

population data and the solar cycle. This clearly showed that the relationship between the solar cycle and lynx abundance is mostly non-significant, except during the time period 1821–1840. For porcupines, however, the relationship with the solar cycle is clear and highly significant (see also Klvana et al. 2004). This example clearly shows how wavelet analyses can contribute to a debate based on complex biological relationships evolving through time.

Discussion

Wavelet analysis can help us to interpret multi-scale, non-stationary time-series data and reveals features we could not see otherwise. Wavelet analysis is thus becoming an important addition to the set of tools used to analyze time series, and thus has important practical applications in environmental sciences.

The major aims of much current research in ecology are to characterize and to understand the nature of order in natural systems, the role of endogenous mechanisms and the influence of exogenous changes on the dynamics of natural systems. As the achievement of these experiments is particularly difficult, retrospective approaches are frequently employed with the use of time-series analysis. Retrospective approaches use a mode of analysis which is rooted in the comparative and observational richness of the data. In consequence, a key requirement is to take into account the major characteristics of the observations that mirror the underlying properties of the studied system. As stressed in the Introduction, transient dynamics appear to be the rule rather than the exception in nature, either because ecological processes are influenced by exogenous trends or because complex endogenous dynamics predominate (e.g., Cushing et al. 1998 or Cazelles 2001). This makes it inappropriate to use traditional techniques when analyzing time series or their mutual dependencies. Using the wavelet approach, we have shown that it is possible to study irregular, non-stationary and noisy time series, and also to analyze weak and transient interactions between such series. The wavelet power spectrum allows quantification of the main periodic component of a given time series and its evolution through time. Dynamic evolution or marked changes can be identified and then associated with endogenous and/or exogenous mechanisms. Wavelet coherency is used to quantify the degree of linear relationship between two non-stationary series in the time–frequency domain. The key advantage of the wavelet approach over the more classic techniques is that it does not share their particularly restrictive requirement of an assumption of stationarity, where all moments of the time series must be constant in time (see also Rodriguez-Arias and Rodó 2004). One of our main results stressed that ecological time series can change dramatically with time. The results from classic approaches must then be interpreted with caution. Furthermore wavelet analysis provides a natural way to follow gradual changes in the forcing by exogenous variables such as environmental or climatic variables.

In practice, wavelet analysis emphasizes interpretation of time series that are changing over time, with good time–frequency localization and the "zoom-in, zoom-out" property, an issue which classic spectral analysis is incapable of addressing. The main advantage of the wavelet approach is clearly to have the possibility to analyze transient dynamics, both to characterize a one-dimensional signal and the association between two time series. As with other classic time-series approaches, inferential methods are needed to characterize the cyclical features of non-stationary time series, and to quantify the relationships between such time series. We have suggested statistical significance tests based on resampling techniques for the "wavelets-based quantities". An important question that is frequently raised by users of the wavelet approach is the number of data points needed for such analysis. We have demonstrated on a short and noisy time series that halving the data points modifies only slightly the conclusions drawn based on the wavelet approach (Fig. 5). The criteria for applying wavelet analysis should thus be very similar to those employed with classic spectral methods. For instance, Murdoch et al. (2002) have analyzed "cyclic species", with a classic spectral method applied to more than 100 time series. They have used a minimum time-series length of 25 years with an estimated period smaller than one-third of the series length as criteria to apply a spectral analysis. Based on our experience, we suggest criteria a little more restrictive than those of Murdoch et al. (2002): time series of 30–40 data points with significant periodic components smaller than 20–25% of the series length. Another interesting aspect is the possibility of easily extracting the phases of the studied signals and then conducting a phase analysis. Phase analysis is a non-linear technique that has a major advantage over linear ones in that it enables the study of rather weak interactions (Cazelles and Stone 2003).

Despite its advantages, the continuous wavelet approach also has its shortcomings. The first one concerns the edge effects at the beginning and at the end of the time series. One way to decrease edge effects is to pad time series with sufficient zeros (Torrence and Compo 1998), but it is impossible to eliminate edge effects, and the region affected by edge effects is known as the "cone of influence". As we have already stressed, the spectral information within this cone is likely to be less accurate. Nevertheless, it is dependent on the mother wavelets that are used. For instance, the Morlet wavelet is more affected by edge effects than is the Mexican hat wavelet (e.g., Torrence and Compo 1998). Even if wavelet analysis performs decomposition with different time supports for different frequencies (see Fig. 1), unfortunately one cannot achieve an arbitrarily high resolution in both the frequency and time domains. Generally, the more accurate the temporal localization of a component is, the less accurate the spectral measure (and vice versa). For example, the Mexican hat wavelet allows for good temporal resolution but poor frequency resolution, whereas the Morlet wavelet allows for good frequency resolution but less precise temporal resolution (e.g., Mi et al. 2005). Therefore, the major consideration in choosing a wavelet is the trade-off between strong localization, which is good for analyzing sharp transients, and weak localization, which induces more precise isolation of dominant frequencies (Lau and Weng 1995).

As a statistical analysis, the wavelet approach provides no information about the underlying ecological mechanisms. There is not a single relation, either between cyclical features and biological mechanisms, or between associations or relationships and mechanisms—a given pattern of association between series may be generated by a wide variety of different mechanisms. For example, we have shown that porcupine populations are phase-locked to the oscillations of solar activity (Fig. 8e–g). Nevertheless, we have not proved that solar cycles are the only factor accounting for the porcupine oscillations. Solar cycles and climatic fluctuations may trigger and/or amplify such population cycles. Further experimental studies will be necessary to elucidate the mechanisms that underlie the phase dependence between population abundance and climatic signals. Like other correlative approaches (e.g., Rodriguez-Arias and Rodó 2004), wavelet analysis must be complemented by experimental tests. However, this technique does provide useful clues about the nature of the underlying ecological processes. Such clues pave the way for future modeling approaches in which explicit mechanisms can be incorporated. In this sense wavelet analysis appears as a spectral technique that may supplement the classic time-series models (e.g., Royama 1992, Ives et al. 2003). Nevertheless, these classic modeling approaches must also take into account these non-stationary features of population systems, for example with time-varying parameters. In this context, Bayesian approaches appear very appealing (e.g., Cazelles and Chau 1997 or Bierman et al. 2006).

Since there are some applications of the DWT in ecology, at least for spatial pattern analysis, one can also compare continuous to discrete wavelet approaches. The main property of the wavelet transform is its ability to provide a time-scale localization of a signal's variance, which derives from the compact support of its basis function. Therefore, wavelet analysis is mainly used with two aims: extraction of local time-scale or time–frequency information, and representation of processes on appropriate bases. Clearly, continuous wavelets are well suited to the first and discrete wavelets for to second aim. Indeed, one of the major advantages of continuous versus discrete wavelets is the well-defined relationship between frequency and scale of continuous wavelets. This greatly facilitates the comparison with Fourier analysis and the analysis of transient phenomena. For the discrete wavelets, this relationship between scale and frequency has less meaning and should be ignored (Daubechies 1992). One disadvantage of the continuous wavelets is that it is characterized by a redundancy of information among the wavelet coefficients. This redundancy implies correlation between coefficients, which is intrinsic to the wavelet function and not to the analyzed time series. The wavelet coefficient interpretation is then strongly dependent on the chosen projection basis, which must be adapted to the specific problem at hand. On the other hand, discrete wavelets that are orthogonal have the ability to concentrate the variance of the signal in a limited number of coefficients. DWT allow a decomposition of a time series in terms of scales—fast and slow scales, for example. The discrete wavelet power spectrum and cross-spectrum have proved to be valuable alternative representations of the variance–covariance distributions across scales (Bradshaw and Spies 1992; Keitt and Urband 2005). Nevertheless, as this scale decomposition is computed on a dyadic base (the number of scale is always 2^n), the number of data points heavily influences this decomposition and particularly the variance repartition (see Fig. 9). Even if analyzing data in a scale-dependent manner is particularly helpful in numerous situations, it is also important to interpret the obtained scales. For example, even if the DWT allow us to identify a shift toward multi-annual variation it can be interesting to explain this shift in terms of frequency to associate this shift with some exogenous forcing. Unfortunately the scale decomposition based on discrete wavelets is difficult to interpret, especially concerning their time evolution (see Fig. 9). This interpretation requires the use of other techniques, contrary to the continuous wavelet transform for which a well-defined relationship between scale and frequency exists.

Recently, another decomposition method has been introduced: the empirical mode decomposition (EMD) (Huang et al. 1998). This method decomposes a time series into different modes similarly to discrete wavelet transform or singular spectrum analysis (Vautard et al. 1992). However, this decomposition uses functions that are data-driven and connected to the local maxima and minima of the time series. This method seems to have similar weaknesses to DWT, which are sensitive to the number of data points and lack of characterization of the different modes (see Fig. 9). This approach has been employed by Cummings et al. (2004) to analyze the spatio-temporal dynamics of dengue incidence in Thailand. Using this technique they observed waves in a 3-year periodic component for Thailand. Nevertheless, they were not able to underline either the transient nature of these waves or their association with large climatic oscillation using this EMD approach, contrary to analyses that have employed continuous wavelet transform (Cazelles et al. 2005).

We have performed a decomposition of non-stationary time series with DWT and EMD to facilitate the comparison with continuous wavelet transforms adopted in this work. We have employed the AR(2) model time series (Eq. 11) used for Fig. 5. Our results, presented in Fig. 9, can easily be compared with those obtained with the continuous wavelet approach (Fig. 5). These results clearly illustrate the main disadvantages of DWT and EMD decompositions, namely that the computed decomposed

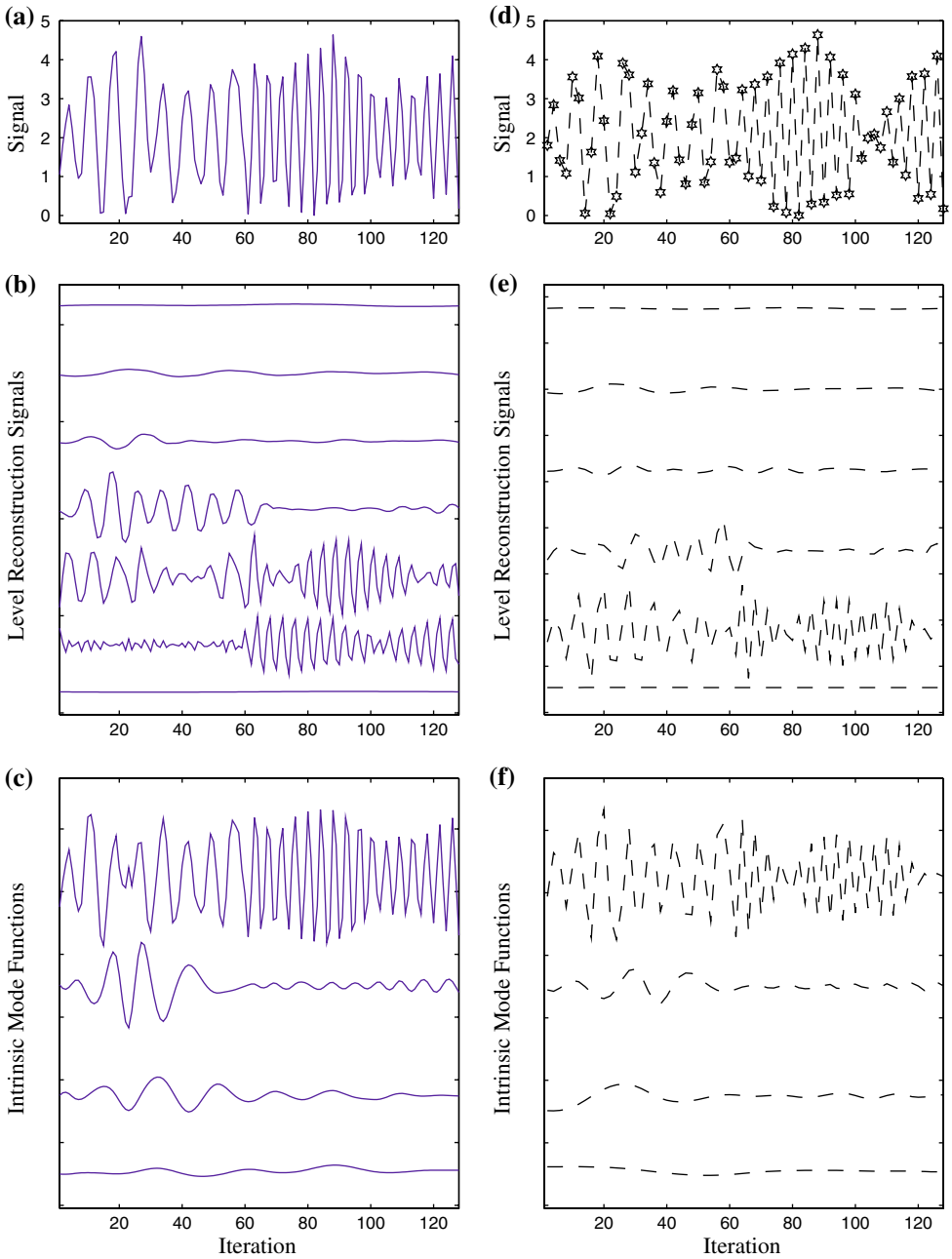

Fig. 9 Comparison between different time-scale decompositions. The analyzed signal is the AR(2) model time series of Fig. 5; however, due to the characteristics of the methods employed [discrete wavelet transforms (DWT) and empirical mode decomposition (EMD)], $2^7 = 128$ data points have been used (**a**). The odd points (64 data points) have also been analyzed (**d**). **b, e** Reconstruction signals from DWT with Daubechies 10 wavelets for the full data set and the odd data points, respectively. The first reconstruction level is at the *top* and the last at the *bottom*. **c**, **f** Intrinsic model functions obtained with EMD for the full data set and the odd data points, respectively. The first intrinsic model function is at the *top* and the fourth at the *bottom*

signals that contain the major part of the variance are non-stationary, as are the analyzed signals (Fig. 9). For instance, the first intrinsic mode function has the same complexity as the raw signal (Fig. 9c, f) and the fourth and fifth levels of reconstruction signals show a marked shift around $t_s = 60$ (Fig. 9b, e). These decompositions (DWT and EMD) then do not permit direct quantification of the time evolution of the main characteristics of the analyzed time series, however crucial for non-stationary signals. These results (Fig. 9b, e) also stress the high sensitivity of the DWT decomposition to the number of data points, contrary to the continuous wavelet approach.

Despite its interesting features, illustrated by our work, wavelet approaches can be improved in different ways. In an ecological context two points warrant further improvement: the irregular or uneven sample data, and the multivariate analysis of time series. As regards awkward sampling quality, Keitt and Fischer (2006), analyzing the response of zooplankton communities to anthropogenic disturbance, employed an adaptive "second-generation" wavelet named the "lifting scheme" (Sweldens 1998). These discrete wavelets have the advantage of adapting their shape near sampling gaps and boundaries. This is an important consideration for ecological time series which

are often short, irregularly sampled and may contain missing values. It will also be interesting to explore the possibility of Foster's wavelet analysis technique (Foster 1996), an appropriate tool for investigating temporarily changing spectral properties of records characterized by uneven sampling quality. The coupling between wavelet analysis and clustering approaches seems a promising avenue for analyzing multivariate time series. The wavelet power spectra could be compared with procedures based on multivariate methods like maximum covariance analysis that was originally used to compare spatio-temporal fields (Rouyer et al. 2008).

Up to very recently, all time-series analyses reported in the ecological literature were based on the stationarity assumption of the data. Some exceptions have been published recently (Grenfell et al. 2001; Rodó et al. 2002; Haydon et al. 2003; Cazelles and Stone 2003; Cazelles 2004; Rodriguez-Arias and Rodó 2004). We hope that our presentation of wavelet analysis promotes a methodological shift in the analysis of ecological time series. Such methodological advances are critical for a better understanding of ecological processes in a rapidly changing global environment.

Acknowledgments We thank the anonymous referees who helped to improve the quality and the clarity of this work. B. C., F. M. and S. J. are partially supported by the program REMIGE–ANR Biodiversité 2005-011.

References

Barbraud C, Weimerskirch H (2001) Emperor penguins and climate change. Nature 411:183–186

Bartlett MS (1954) Problèmes de l'analyse spectrale des séries temporelles stationnaires. Publ Inst Stat Univ Paris 3:119–134

Benton TG, Plaistow SJ, Coulson TN (2006) Complex population dynamics and complex causation: devils, details and demography. Proc R Soc Lond B 273:1173–1181

Bierman SM, Fairbairn JP, Petty SJ, Elston DA, Tidhar D, Lambin X (2006) Changes over time in the spatiotemporal dynamics of cyclic populations of field voles (*Microtus agrestis* L.). Am Nat 167:583–590

Bjørnstad ON, Grenfell BT (2001) Noisy clock: time series analysis of population fluctuations in animals. Science 293:638–643

Bradshaw GA, Spies TA (1992) Characterizing canopy gap structure in forest using wavelet analysis. J Ecol 80:205–215

Buonaccorsi JP, Elkinton JS, Evans SR, Liebhold AM (2001) Measuring and testing spatial synchrony. Ecology 82:1628–1679

Cazelles B (2001) Blowout bifurcation with non-normal parameters in population dynamics. Phys Rev E 64:032901

Cazelles B (2004) Symbolic dynamics for identifying similarity between rhythms of ecological time series. Ecol Lett 7:755–763

Cazelles B, Chau NP (1997) Using the Kalman filter and dynamic models to assess the changing HIV/AIDS epidemic. Math Biosci 140:131–154

Cazelles B, Hales S (2006) Infectious diseases, climate influences and nonstationarity. PLoS Med 3:1212–1213 (e328)

Cazelles B, Stone L (2003) Detection of imperfect population synchrony in an uncertain world. J Anim Ecol 72:953–968

Cazelles B, Bottani S, Stone L (2001) Unexpected coherence and conservation. Proc Royal Soc Lond B 268:2595–2602

Cazelles B, Chavez M, McMichael AJ, Hales S (2005) Nonstationary influence of El Niño on the synchronous dengue epidemics in Thailand. PLoS Med 2:313–318 (e106)

Chatfield JR (1989) The analysis of time series: an introduction. Chapman & Hall, London

Cummings DAT,, Irizarry RA, Huang NE, Endy TP, Nisalak A, Ungchusak K, Burke DS (2004) Travelling waves in the occurrence of dengue haemorrhagic fever in Thailand. Nature 427:344–347

Cushing JM, Dennis B, Desharnais RA, Costantino RF (1998) Moving toward an unstable equilibrium: saddle nodes in population systems. J Anim Ecol 67:298–306

Dale MRT, Mah M (1998) The use of wavelets for spatial pattern analysis in ecology. J Veg Sci 9:805–815

Daubechies I (1992) Ten lectures on wavelets. SIAM monographs, Philadelphia

Duncan CJ, Duncan SR, Scott S (1996) Whooping cough epidemics in London, 1701–1812: infection dynamics, seasonal forcing and the effects of malnutrition. Proc R Soc Lond B 263:445–450

Efron B, Tibshirani RJ (1993) An introduction to the bootstrap. Chapman & Hall, London

Elton CS (1924) Fluctuations in the numbers of animals, their causes and effects. Br J Exp Biol 2:119–163

Elton CS, Nicholson M (1942) The ten-year cycle in numbers of the lynx in Canada. J Anim Ecol 11:215–244

Forchhammer MC, Post E (2004) Using large-scale climate indices in climate change ecology studies. Popul Ecol 46:1–12

Foster G (1996) Wavelets for period analysis of unevenly sampled time series. Astronom J 112:1709–1729

Gabor D (1946) Theory of communication. J Inst Electr Eng 93:429–457

Grenfell BT, Bjørnstad ON, Kappey J (2001) Travelling waves and spatial hierarchies in measles epidemics. Nature 414:716–723

Hare SR, Mantua NJ (2000) Empirical evidence for North Pacific regime shifts in 1997 and 1989. Prog Oceanogr 47:103–145

Hastings A (2001) Transient dynamics and persistence of ecological systems. Ecol Lett 4:215–220

Haydon DT, Greenwood PE, Stenseth NC, Saitoh T (2003) Spatiotemporal dynamics of the grey-sided vole in Hokkaido: identifying coupling using state-based Markov-chain modelling. Proc R Soc Lond B 270:435–445

Huang NE, Shen Z, Long SR, Wu MC, Shih HH, Zheng Q, Yen NC, Tung CC, Liu HH (1998) The empirical mode decomposition and the Hilbert spectrum for nonlinear and non-stationary time series analysis. Proc R Soc Lond A 454:903–995

Ives AR, Dennis B, Cottingham KL, Carpenter SR (2003) Estimating community stability and ecological interactions from time series data. Ecol Monogr 73:301–330

Jenouvrier S, Weimerskirch H, Barbraud C, Park YH, Cazelles B. (2005) Evidence of a shift in the cyclicity of Antarctic seabirds dynamics linked to climate. Proc R Soc Lond B 272:887–895

Johnson DM, Bjørnstad ON, Liebhold AM (2006) Landscape mosaic induces traveling waves of insect outbreaks. Oecologia 148:51–60

José MV, Bishop RF (2003) Scaling properties and symmetrical patterns in the epidemiology of rotavirus infection. Phil Trans R Soc Lond B 358:1625–1641

Keitt TH, Fischer J (2006) Detection of scale-specific community dynamics using wavelets. Ecology 87:2895–2904

Keitt TH, Urband DL (2005) Scale-specific inference using wavelets. Ecology 86:2497–2504

Klvana I, Berteaux D, Cazelles B (2004) Porcupine feeding scars and climatic data show ecosystem effects of the solar cycle. Am Nat 164:283–297

Koelle K, Pascual M (2004) Disentangling extrinsic from intrinsic factors in disease dynamics: a nonlinear time series approach with an application to cholera. Am Nat 163:901–913

Lau KM, Weng H (1995) Climatic signal detection using wavelet transform: how to make a time series sing. Bull Am Meteorol Soc 76:2391–2402

Liebhold AM, Koening WD, Bjørnstad ON (2004) Spatial synchrony in population dynamics. Annu Rev Ecol Evol Syst 35:467–490

Liu PC (1994) Wavelet spectrum analysis and ocean windwaves. In: Foufoula-Georgiou E, Kumar P (eds) Wavelets in geophysics. Academic Press, New York, pp 151–166

Mackenzie JMD (1952) Fluctuations in the number of British tetraonids.J Anim Ecol 21:128–153

Mallat S (1998) A wavelet tour of signal processing. Academic Press, San Diego

Ménard F, Marsac F, Bellier B, Cazelles B (2007) Climatic oscillations and tuna catch rates in the Indian Ocean: a wavelet approach to time series analysis. Fish Oceanogr 16:95–104

Meyers SD, Kelly BG, O'Brien JJ (1993) An introduction to wavelet analysis in oceanography and meteorology with application to the dispersion of Yanai waves. Mon Weather Rev 121:2858–2866

Mi X, Ren H, Ouyang Z, Wei W, Ma K (2005) The use of the Mexican hat and the Morlet wavelets for detection of ecological patterns. Plant Ecol 179:1–19

Murdoch WW, Kendall BE, Nisbet RM, Briggs CJ, McCauley E, Bolser R (2002) Single-species models for many-species food webs. Nature 423:541–543

Nezlin NP, Li BL (2003) Time-series analysis of remoted-sensed chlorophyll and environmental factors in the Santa Monica-San Pedro basin off Southern California. J Mar Syst 39:185–202

Pikovsky AS, Rosenblum MG, Kurths J (2001)Synchronization: a universal concept in nonlinear sciences.Cambridge University Press, Cambridge

Platt T, Denman KL (1975) Spectral analysis in ecology. Annu Rev Ecol Syst 6:189–210

Reid PC, Borges MF, Svendsen E (2001) A regime shift in the North Sea circa in 1988 linked to changes in the North Sea horse mackerel fishery. Fish Res 50:163–171

Rodó X., Pascual M, Fuchs G, Faruque SG (2002) ENSO and cholera: a nonstationary link related to climate change? Proc Natl Acad Sci USA 99:12901–12906

Rodriguez-Arias MA, Rodó X (2004) A primer on the study of transitory dynamics in ecological series using the scaledependent correlation analysis. Oecologia 138:485–504

Rohani P, Earn DJD, Grenfell BT (1999) Opposite patterns of synchrony in sympatric disease metapopulations. Science 286:968–971

Rohani P, Green CJ, Mantilla-Beniers NB, Grenfell BT (2003) Ecological interference between fatal diseases. Nature 422:885–888

Rosenberg M (2004) Wavelet analysis for detecting anisotropy in point patterns. J Veg Sci 15:277–284

Rouyer T, Fromentin JM, Stenseth NC, Cazelles B (2008) Analysing multiple time series and extending significance testing in wavelet. Mar Ecol Progr Ser (in press)

Royama T (1992) Analytical population dynamics. Chapman & Hall, London

Saitoh T, Cazelles B, Vik JO, Viljugrein H, Stenseth NC (2006) Effects of the regime shift on population dynamics of the grey-sided vole in Hokkaido, Japan. Clim Res 32:109–118

Sinclar ARE, Gosline JM, Holdsworth G, Krebs CJ, Boutin S, Smith JNM, Boonstra R, Dale M (1993) Can the solar cycle and climate synchronize the snowshoe hare cycle in Canada? Evidence from the tree rings and ice cores. Am Nat 141:173–198

Stenseth NC, Mysterud A, Ottersen G, Hurrel JW, Chan KS, Lima M (2002) Ecological effects of climate fluctuations. Science 297:1292–1296

Sweldens W (1998) The lifting scheme: a construction of second generation wavelets. SIAM J Math Anal 29:511–546

Theiler J, Eubank S, Longtin A, Galdrikian B, Farmer JD (1992) Testing for nonlinearity in time series: the method of surrogate data. Physica D 58:77–94

Torrence C, Compo GP (1998) A practical guide to wavelet analysis. Bull Am Meteorol Soc 79:61–78

Vautard R, Yiou P, Ghil M (1992) Singular spectrum analysis: a toolkit for short, noisy chaotic signals. Physica D 58:95–126

Xia Y, Bjørnstad ON, Grenfell BT (2004) Measles metapopulation dynamics: a gravity model for epidemiological coupling and dynamics. Am Nat 164:267–281